

Temperature-triggered formation of a cellulose II nanocrystal network through regioselective derivatization

Fangbo LIN, Frédéric PIGNON, Jean-Luc PUTAUX, and Bruno JEAN

Electronic Supplementary Information

Wide-angle X-ray scattering (WAXS). Lyophilized CNC powders were pressed into a thin film and X-rayed in a Warhus vacuum chamber using a Philips PW3830 generator operating at 30 kV and 20 mA (Ni-filtered CuK α radiation, $\lambda = 0.1542$ nm). Two-dimensional diffraction patterns were recorded on Fujifilm imaging plates, read offline with a Fujifilm BAS 1800-II bioimaging analyzer. Profiles were calculated by rotational averaging of the 2D patterns.

Fourier-transform infrared spectroscopy (FTIR). FTIR spectra of CNC-I and CNC-II were recorded on a Perkin-Elmer spectrum 65 (PerkinElmer, USA) between 400 and 4000 cm $^{-1}$ with a resolution of 1 cm $^{-1}$ and 16 scans were acquired. Attenuated total reflectance (ATR) mode was used on all samples and baseline correction was applied. The spectra were normalized at 1160 cm $^{-1}$.

^{13}C CP/MAS nuclear magnetic resonance spectroscopy (CP/MAS NMR). CP/MAS NMR spectra were recorded with a Bruker Avance DSX 400 MHz spectrometer, in a cross-polarization and magic angle spinning conditions (CP-MAS). The ^{13}C radio frequency field strength was obtained by matching the Hartman-Hahn conditions at 60 kHz. The spinning speed was 12000 Hz, the operating condition was set at 100.6 MHz and a minimum number of 2000 of scans were integrated with a contact time of 2 ms using a ramp CP protocol and a recycle delay of 2 s. The acquisition time was 35 ms and the sweep width set at 29400 Hz. The chemical shifts were calibrated with respect to the carbonyl peak of glycine (176.03 ppm). The spectra were normalized with the peak of carbon C1 of cellulose between 100 to 110 ppm.

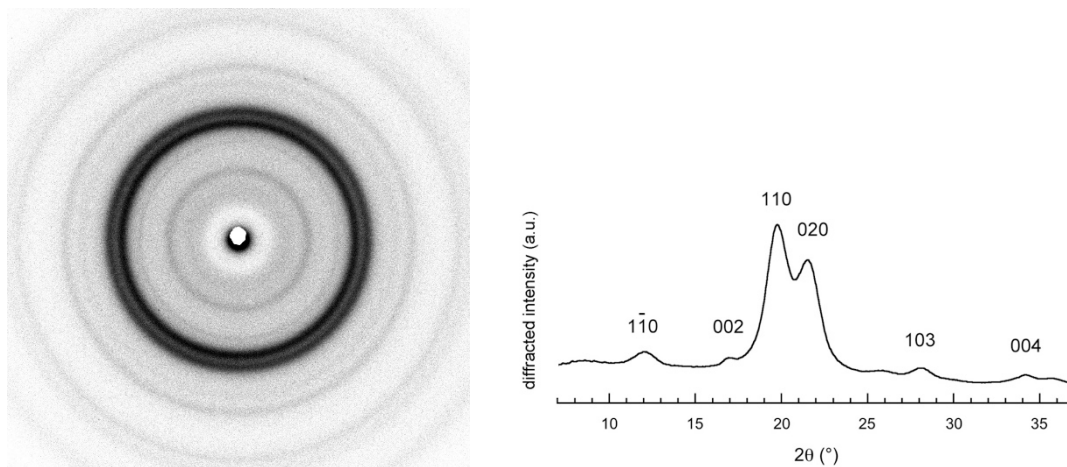


Figure S1. X-ray powder diffraction pattern of freeze-dried cellulose II cotton nanocrystals and corresponding peak indexing.

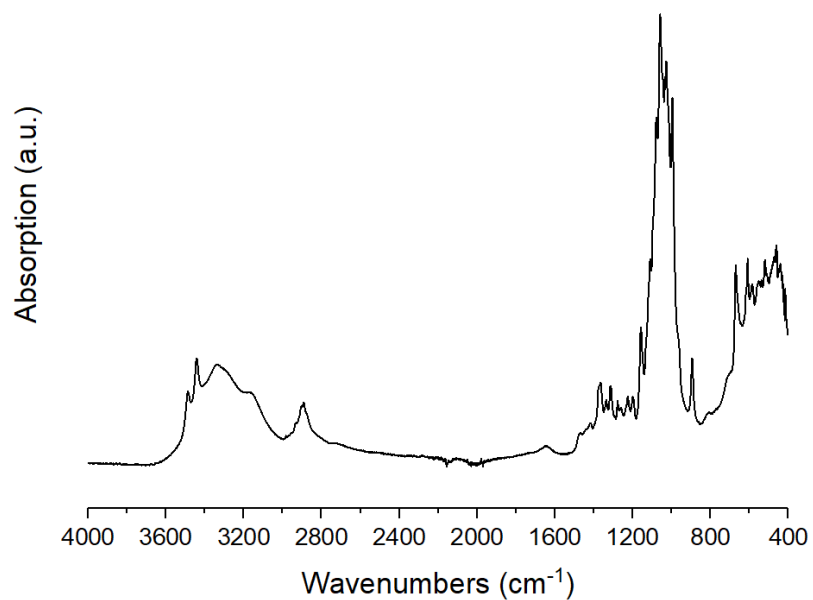


Figure S2. FTIR spectrum of freeze-dried cotton cellulose II nanocrystals.

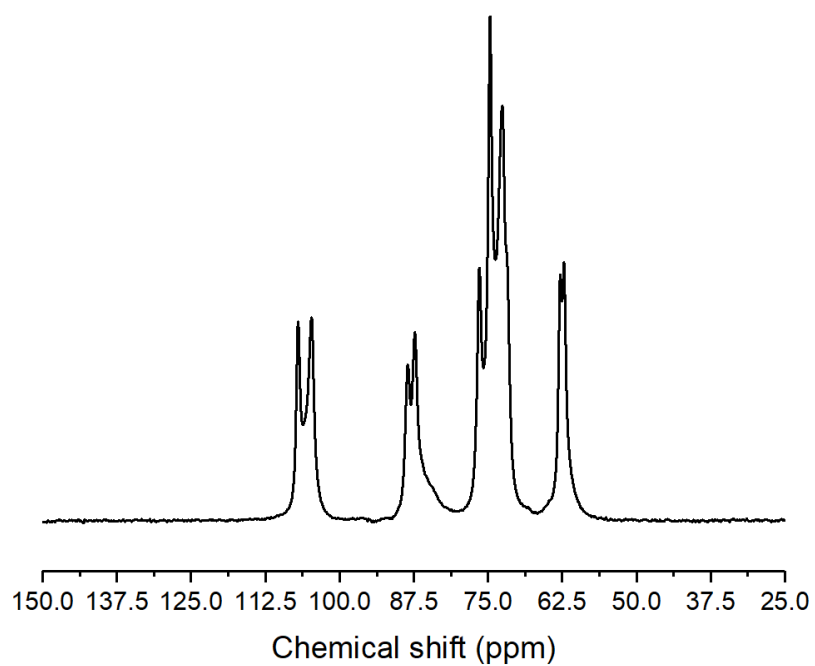


Figure S3. ^{13}C CP/MAS NMR spectrum of freeze-dried cotton cellulose II nanocrystals.

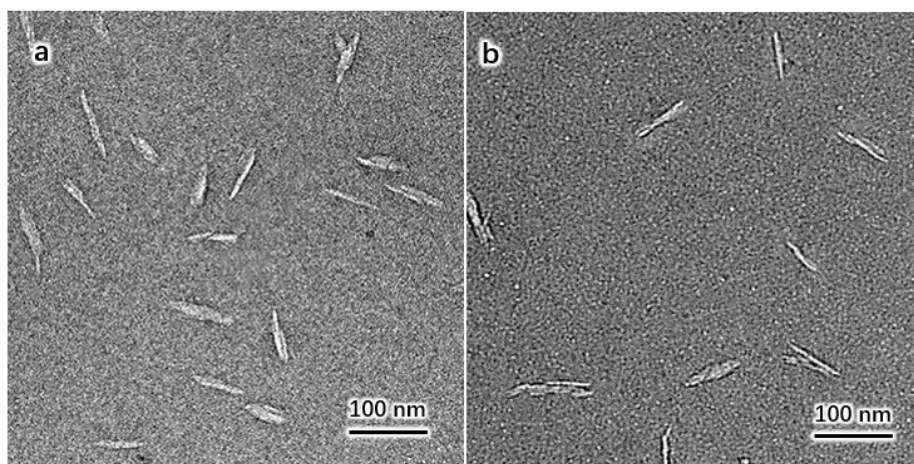


Figure S4. TEM images of negatively stained T5000-e-CNC-II particles from an aqueous suspension kept at 4 °C (a) and cooled down from 24 to 4 °C (b).

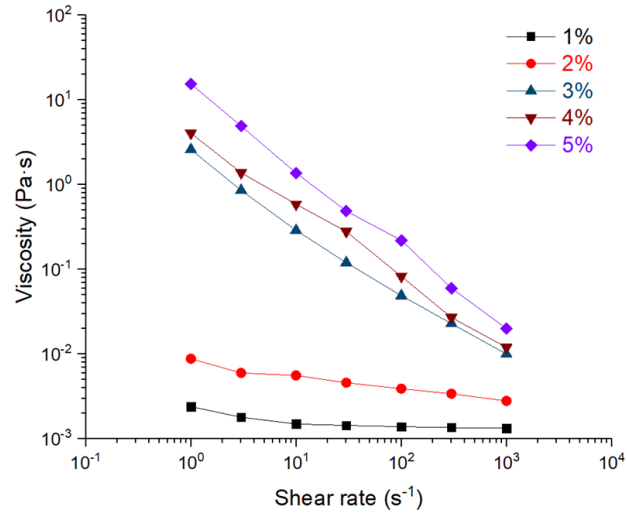


Figure S5. Flow curves of CNC-II aqueous suspensions at a concentration of 1, 2, 3, 4 and 5 wt % within a shear rate ranging from 1 to 1000 s^{-1} .

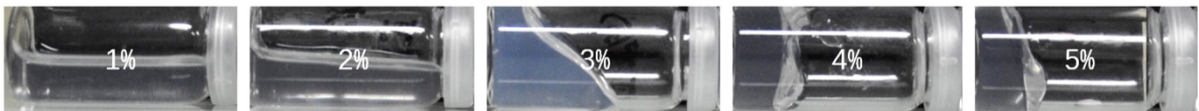


Figure S6. Photographs of CNC-II aqueous suspensions in horizontal vials at room temperature. Their concentration varies from 1 to 5 wt %.

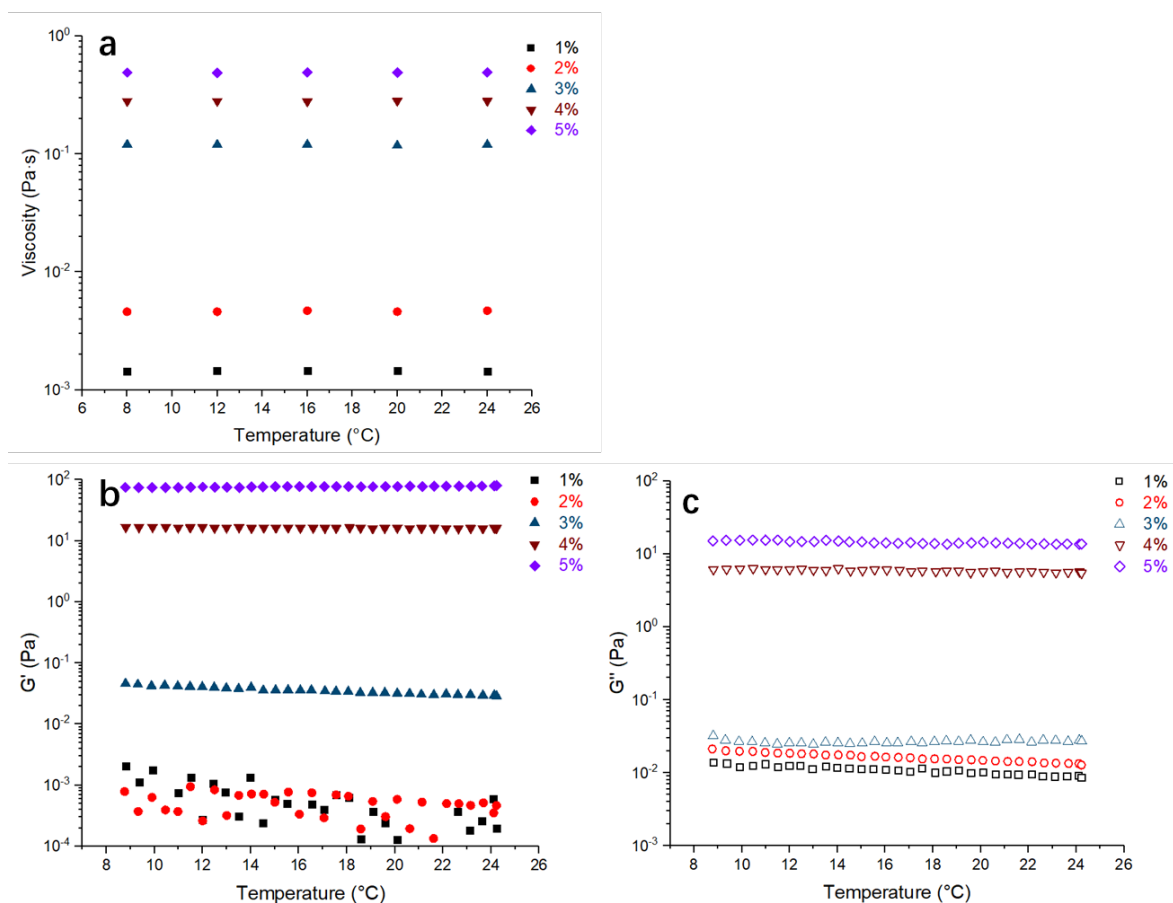


Figure S7. a) Viscosity as a function of temperature within the 8-24 °C range for CNC-II aqueous suspensions at a concentration of 1, 2, 3, 4 and 5 wt % and at a shear rate of 30 s^{-1} . b) Storage modulus G' and c) loss modulus G'' as a function of temperature of CNC-II samples. Experiments were performed within a temperature range between 8 and 24 °C at a 0.01 strain and an angular frequency of 1 Hz for 2 to 5 wt % suspensions and at a 0.02 strain for the 1 wt % suspension owing to its fluidity.

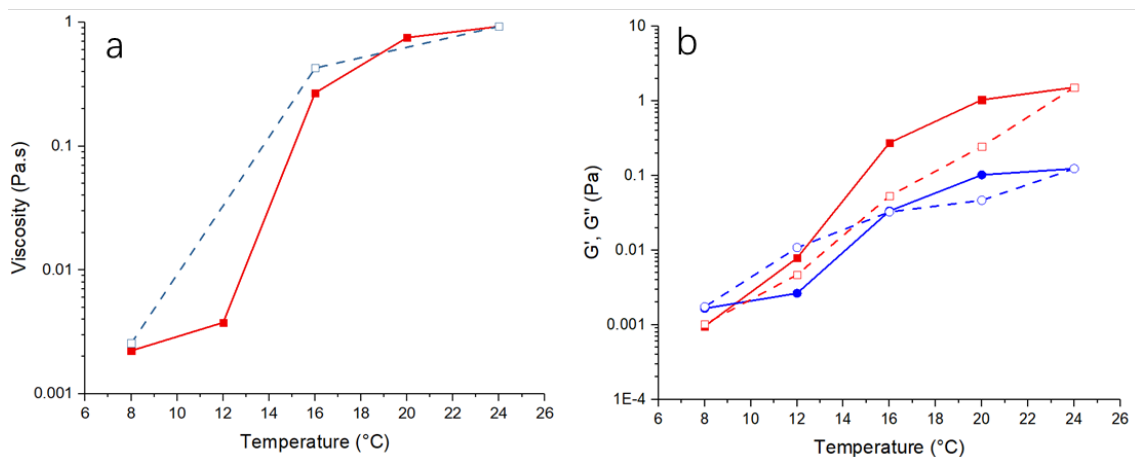


Figure S8. a) Viscosity of a 1 wt % T5000-e-CNC-II sample during a 8-24 °C temperature cycle (heating: red squares and continuous line, and cooling: blue dots and dashed line) at a shear rate of 30 s^{-1} ; b) Storage modulus G' (red square) and loss modulus G'' (blue dot) of a 1 wt % T5000-e-CNC-II sample during a 8-24 °C temperature cycle (heating: red squares and continuous line, and cooling: blue dots and dashed line) at 0.01 strain and an angular frequency of 1 Hz.

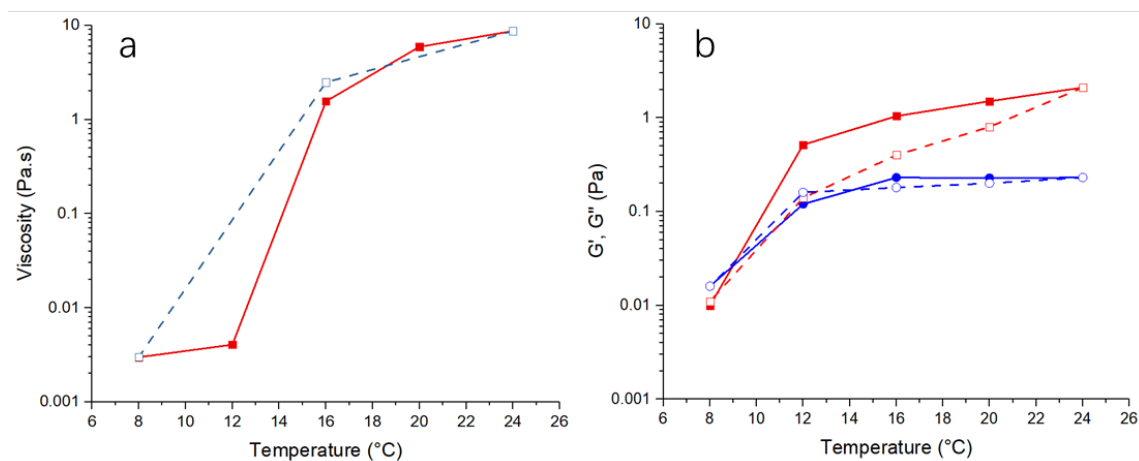


Figure S9. a) Viscosity of a 2 wt % T5000-e-CNC-II sample during a 8-24 °C temperature cycle (heating: red squares and continuous line, and cooling: blue dots and dashed line) at a shear rate of 30 s^{-1} ; b) Storage modulus G' (red square) and loss modulus G'' (blue dot) of a 2 wt % T5000-e-CNC-II sample during a 8-24 °C temperature cycle (heating: red squares and continuous line, and cooling: blue dots and dashed line) at 0.01 strain and an angular frequency of 1 Hz.

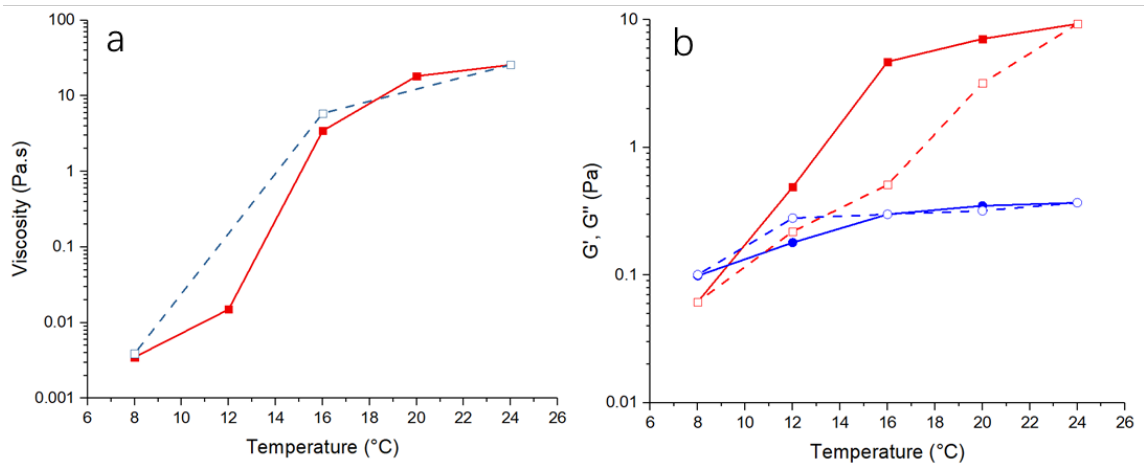


Figure S10. a) Viscosity of a 3 wt % T5000-e-CNC-II sample during a 8-24 °C temperature cycle (heating: red squares and continuous line, and cooling: blue dots and dashed line) at a shear rate of 30 s^{-1} ; b) Storage modulus G' (red square) and loss modulus G'' (blue dot) of a 3 wt % T5000-e-CNC-II sample during a 8-24 °C temperature cycle (heating: red squares and continuous line, and cooling: blue dots and dashed line) at 0.01 strain and an angular frequency of 1 Hz.

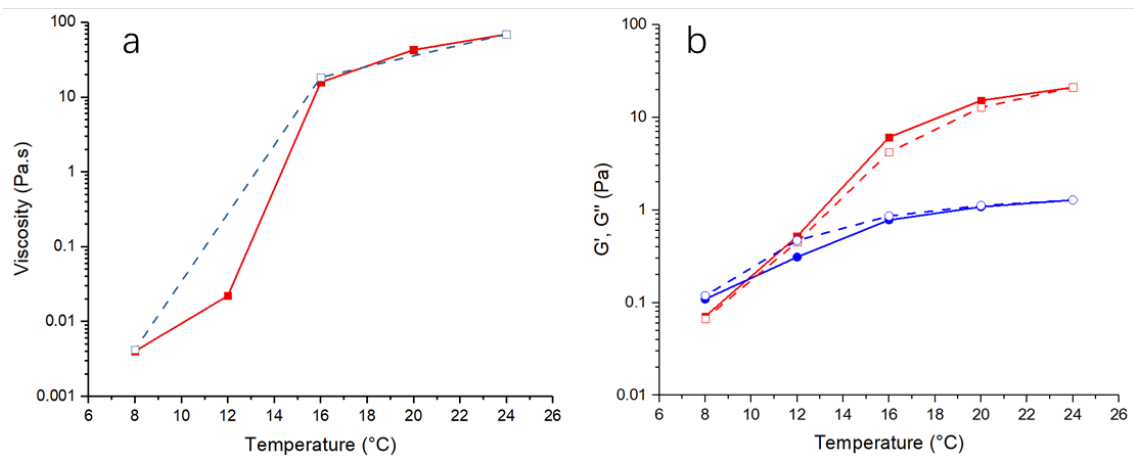


Figure S11. a) Viscosity of a 4 wt % T5000-e-CNC-II sample during a 8-24 °C temperature cycle (heating: red squares and continuous line, and cooling: blue dots and dashed line) at a shear rate of 30 s^{-1} ; b) Storage modulus G' (red square) and loss modulus G'' (blue dot) of a 4 wt % T5000-e-CNC-II sample during a 8-24 °C temperature cycle (heating: red squares and continuous line, and cooling: blue dots and dashed line) at 0.01 strain and an angular frequency of 1 Hz.

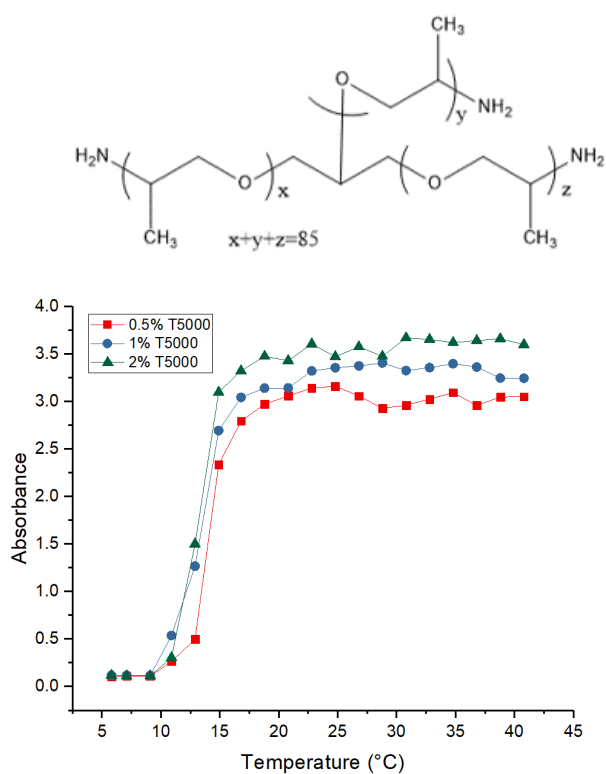


Figure S12. Chemical structure of the Jeffamine® polyetheramine T5000 and UV absorbance spectra of 0.5, 1 and 2 wt % solutions as a function of temperature showing a LCST at around 12 °C.